

# An Open-Source Inversion Algorithm for the Munsell Renotation

Paul Centore

© June 2011

## Abstract

*The 1943 Munsell renotation includes a table that converts 2,734 Munsell specifications into  $xyY$  coordinates, along with a graphical interpolation method, and a graphical inversion method, that converts  $xyY$  coordinates back into Munsell specifications. The current paper presents open-source computer code, running in Matlab or Octave, that both interpolates and inverts the Munsell renotation automatically. The steps in both algorithms are described in detail. Like previous inversion algorithms, it relies on interpolations between entries in the 1943 table. For colours near the MacAdam limits, the inversion also requires extrapolations beyond the 1943 entries. The outputs of the current implementation do not differ significantly from the outputs of other inversion algorithms. The main distinguishing feature of the current algorithm is that both the algorithm and code implementation are publicly available.*

**Keywords:** Munsell, renotation, inverse renotation, open source, algorithm

## 1 Introduction

The Munsell colour system classifies object colours by three perceptual properties: hue, value, and chroma. In 1931, the Commission Internationale de l'Éclairage (CIE) used colorimetry to standardize an objective method<sup>1</sup> of specifying when two colour samples are perceptually identical. An important practical problem is to calculate the Munsell coordinates of a colour stimulus from only its CIE specifications. The 1943 Munsell renotation<sup>2</sup> provided empirical data for this undertaking. First, Newhall and his coworkers averaged many observers' colour judgements to produce a smoothed, experimentally sound, version of the 1929 Munsell system. Second, they

measured the smoothed colour samples, producing Table I of the renotation,<sup>2</sup> which specifies 2,734 Munsell samples in CIE coordinates. This work confirmed previous findings that Munsell value is solely a function of luminance factor, denoted  $Y$  in the CIE system. Newhall's renotation table, along with the supporting conditions and methods of calculation, has been incorporated in the ASTM International standard for the Munsell system.<sup>3</sup>

Newhall and coworkers<sup>2</sup> recommended graphical methods for interpolation and inversion in the Munsell renotation. To interpolate is to find the CIE coordinates for an arbitrary Munsell specification, by averaging over the 2,734 renotation points. To invert is to find the Munsell specification for a given set of CIE coordinates. This paper presents algorithms for both interpolation and inversion, as well as an open-source computer code implementation. As of January 2011, the implementation has been submitted to the Colorlab project,<sup>4</sup> and runs in either Matlab or its freely available clone, Octave; the implementation requires some previous Colorlab code. The two main computer routines are `MunsellToxyY.m` and `xyYtoMunsell.m`. If they are not yet in Colorlab, then these routines, along with necessary supporting routines, can be downloaded from [www.99main.com/~centore](http://www.99main.com/~centore).

The interpolation and inversion algorithms presented here produce similar output to previous algorithms such as those by Rheinboldt,<sup>5</sup> Simon & Frost,<sup>6</sup> ASTM,<sup>3</sup> Wallkill,<sup>7</sup> and BabelColor.<sup>8</sup> Descriptions of the algorithms in the first three references have been published, but no computer implementation is publicly available. Smith, Whitfield, & Wiltshire<sup>9</sup> mention a Pascal implementation of Rheinboldt's algorithm, freely available for non-commercial use, but this implementation could not be located. The fourth and fifth references are commercial computer programs which convert a user's entries from Munsell to CIE coordinates, and vice versa; the code for these programs is not publicly available, however, and neither are descriptions of the underlying algorithms.

The current work was motivated by an investigation of shadow colours, which required about 1500 inversions. Graphically inverting 1500 CIE triples was prohibitive, as was manual entry into a program such as Wallkill. Though BabelColor's Patch-Tool can convert text files of arbitrary length, it was also desired that the conversion algorithm be explicit. To meet these demands, the algorithms presented here were developed from scratch, as were the computer implementations. The openness of both algorithms and computer code is believed to be unique. Other researchers are invited to use and modify them.

## 2 The Munsell Renotation

Albert Munsell originally defined the Munsell system conceptually. A colour is specified by its hue, value, and chroma. Hue is notated by a number between 0 and 10, which prefixes one of ten hue names: red (R), yellow-red (YR), yellow (Y), green-yellow (GY), green (G), blue-green (BG), blue (B), purple-blue (PB), purple (P), and red-purple (RP). There are a total of 100 hues with integer prefixes. Value, indicating how light a colour is, is a number between 0 (signifying black) and 10 (white). Chroma extends from 0 (grey) to a positive number, which increases to a varying perceptual limit as a colour's difference from a grey, of the same Munsell hue and value, increases. The 100 hues with integer prefixes are evenly spaced perceptually, as are values and chromas. In addition to Munsell's abstract definition, the 1929 *Munsell Book of Color* contained physical exemplifications of Munsell specifications. This book became a physical standard for the system.

The Munsell renotation, incorporated into ASTM Standard D1535-08,<sup>3</sup> defines the Munsell system objectively, by using colorimetry to specify Munsell samples. The Munsell system applies to reflective (i.e. non-self-luminous) colours, that inhere in physical objects, rather than to coloured lights. Illuminant C, at levels characteristic of indirect daylight, was chosen as the standard lighting source. Colorimetric measurements were made of Munsell samples, from which their CIE coordinates were calculated, relative to Illuminant C.

Standardized CIE coordinates were used to express the smoothed colours objectively. In 1931, the CIE defined three colour-matching functions, named  $\bar{x}(\lambda)$ ,  $\bar{y}(\lambda)$ , and  $\bar{z}(\lambda)$ . The domain of the three functions is the visible region of the electromagnetic spectrum, spanning from approximately 360 nm to 760 nm. Illuminant C is given by a spectral power distribution (SPD),  $C(\lambda)$ , with the same domain as the colour-matching functions. Tables I & II of Judd's CIE paper<sup>1</sup> tabulate the colour-matching functions and the Illuminant C SPD.

In contrast to a light source, an object colour is specified by its reflectance spectrum,  $r(\lambda)$ , for the same domain. The function  $r(\lambda)$  takes on values between 0 and 1, or alternately, between 0 and 100 percent. At each wavelength  $\lambda$ , the object reflects  $r(\lambda)$  percent of the quantity  $C(\lambda)$ , which is the portion of the incident light whose wavelength is  $\lambda$ . The SPD of the reflected light is therefore  $r(\lambda)C(\lambda)$ . The relative CIE coordinates for an object colour's reflectance spectrum are

$$X_r = \frac{\int_{360}^{760} \bar{x}(\lambda)r(\lambda)C(\lambda)d\lambda}{\int_{360}^{760} \bar{y}(\lambda)C(\lambda)d\lambda}, \quad (1)$$

$$Y_r = \frac{\int_{360}^{760} \bar{y}(\lambda)r(\lambda)C(\lambda)d\lambda}{\int_{360}^{760} \bar{y}(\lambda)C(\lambda)d\lambda}, \quad (2)$$

$$Z_r = \frac{\int_{360}^{760} \bar{z}(\lambda)r(\lambda)C(\lambda)d\lambda}{\int_{360}^{760} \bar{y}(\lambda)C(\lambda)d\lambda}. \quad (3)$$

Newhall uses a transformation of relative CIE coordinates:

$$x = \frac{X_r}{X_r + Y_r + Z_r}, \quad (4)$$

$$y = \frac{Y_r}{X_r + Y_r + Z_r}, \quad (5)$$

$$Y = Y_r. \quad (6)$$

The variables  $x$  and  $y$  in this coordinate system are thought of as chromaticity coordinates, while  $Y$ , because of the way the CIE defined  $\bar{y}(\lambda)$ , is thought of as an indicator of relative luminance.  $Y$  is called the luminance factor and is alternately expressed as a value between 0 and 1, and as a percentage.

The Munsell system uses hue ( $pH$ ), value ( $V$ ), and chroma ( $C$ ), as coordinates. A Munsell specification is of the form  $pH V/C$ , where  $p$  is a numerical prefix between 0 and 10, that modifies  $H$ . Neutral greys are expressed in the form  $NV$ , where  $V$  is the grey's value. Table I of the renotation<sup>2</sup> converts 2,734 Munsell specifications to  $xyY$  coordinates. The entries in Table I vary over all integer Munsell values from 1 to 9, over all hues prefixed by 2.5, 5.0, 7.5, or 10.0, and over all chromas in even integer steps, from 2 to the MacAdam limits. Although Table I does not list conversions for greys, the chromaticity coordinates of any grey are identical to the neutral point of Illuminant C:

$$x = 0.31006, \quad (7)$$

$$y = 0.31616. \quad (8)$$

The  $Y$  coordinate for a grey of value  $V$  can be read off from Table 1 of the ASTM standard.<sup>3</sup> Mathematically, Newhall's table is a discretization of a function,  $f$ , from  $\{pH, V, C\}$  to  $\{Y, x, y\}$ , given by three subfunctions:

$$Y = f_1(pH, V, C), \quad (9)$$

$$x = f_2(pH, V, C), \quad (10)$$

$$y = f_3(pH, V, C). \quad (11)$$

These three functions define the Munsell renotation.

An important result, expressed in Eq. 2 of the ASTM standard,<sup>3</sup> is that the first function,  $f_1$ , is given by a bijective quintic polynomial that only depends on  $V$ , and not on  $H$  or  $C$  :

$$Y = f_1(V) = 0.00081939V^5 - 0.020484V^4 + 0.23352V^3 - 0.22533V^2 + 1.1914V, (12)$$

where  $V$  is the Munsell value, between 0 and 10, and  $Y$  is a percentage. In perceptual terms, the Munsell value of a colour sample depends only on that sample's luminance factor. The ASTM quintic in Equation (12) is used because it fits empirical data well. It is 0.975 times an earlier quintic on p. 417 of Newhall's renotation paper,<sup>2</sup> which measured the luminance factor with reference to a magnesium oxide standard; the ASTM measures luminance factor with respect to a perfect white diffuser. The ASTM scaling factor makes the Munsell value of 10 correspond to a reflectance factor of 100%.

The problem of interpolation is to find  $xyY$ , for an arbitrary Munsell specification. The problem of inversion is to find, for a given  $xyY$ , a Munsell specification  $\{pH, V, C\}$ , such that  $f(\{pH, V, C\}) = xyY$ . The following sections will present algorithms for interpolation and inversion. The inversion algorithm uses the interpolation algorithm, but interpolation can be performed without reference to inversion.

### 3 Renotation Interpolation

Table I of the renotation<sup>2</sup> presents the Munsell renotation data as a look-up table, that converts Munsell specifications directly to  $xyY$  coordinates. Interpolation, however, is needed for Munsell specifications that are not in Table I. The interpolation will be performed in two steps: interpolation when the Munsell value is an integer, and then interpolation for non-integers.

#### 3.1 Interpolation for an Integer Munsell Value

Since the renotation provides data for integer Munsell values, this section will solve the natural subproblem of interpolating when the Munsell value is an integer. First, curves (ovals and radials) are fit to the renotation data for an integer value, and then those curves are interpolated over.

##### 3.1.1 Constructing Ovals and Radials

Figure 1 plots the  $xy$  coordinates for all colours with Munsell value 4, in Table I of the renotation.<sup>2</sup> Two sets of implicit curves are evident. The first are lines

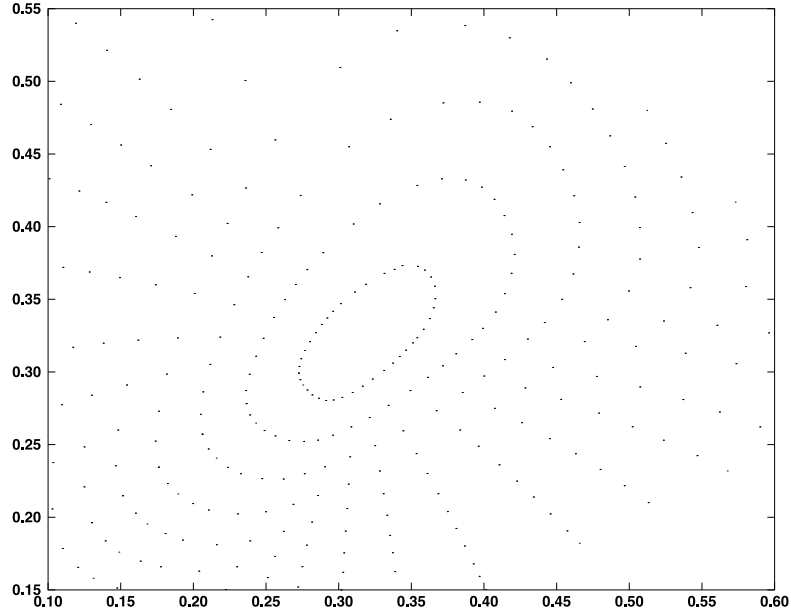


Figure 1: Plot of  $xy$  Coordinates of Colours of Value 4 in Table I of the renotation<sup>2</sup>

that radiate outward from the Illuminant C white point given by Equations (7) and (8). The second are ovoids that are centered approximately on the white point. The radials are lines of constant hue and varying chroma. The ovoids are lines of constant chroma and varying hue. The two kinds of curves intersect at the renotation data. The curves in Figures 1 to 9 of the renotation<sup>2</sup> were manually drawn; they are *ad hoc* curves that are reasonably smooth and go through the renotation points. A mathematical scheme will automate this drawing of radials and ovoids.

The curves' form suggests transforming  $x$  and  $y$  to polar coordinates about the neutral point:

$$x - 0.31006 = r \cos \theta, \quad (13)$$

$$y - 0.31616 = r \sin \theta. \quad (14)$$

Under this coordinate transformation,

$$r = \sqrt{(x - 0.31006)^2 + (y - 0.31616)^2}. \quad (15)$$

The angle  $\theta$  is 0 for the ray through the neutral point, along the positive  $x$ -axis, and is measured counterclockwise from that ray.

Ovoids are drawn through data points of the same chroma in Figure 1, requiring interpolation. While Newhall *et al.* draw smooth curves visually in their Figures 1

through 9, both Rheinboldt and Simon use linear interpolation. In sections of the ovoid where curvature is high, linear interpolation distorts the ovoid's shape.

To avoid this distortion, the current paper uses radial interpolation, about the neutral point, for segments of high curvature. In radial interpolation, two adjacent Munsell data points, of the same chroma, but of consecutive hues, are written in polar coordinates,  $(r_1, \theta_1)$  and  $(r_2, \theta_2)$ . The interpolating line between the data points consists of all points  $(r_3, \theta_3)$ , such that

$$\frac{r_3 - r_1}{r_2 - r_1} = \frac{\theta_3 - \theta_1}{\theta_2 - \theta_1}. \quad (16)$$

If  $(r_1, \theta_1)$  and  $(r_2, \theta_2)$  were two points of a circle centered on the neutral point, then the radial interpolation would be the circular arc joining them. Table 1 lists the segments for which radial interpolation was used; all other segments were interpolated linearly. In the third column, the segment's counterclockwise boundary is listed before its clockwise boundary; for example, the segment 10Y-5YR starts at the hue 10Y, and proceeds clockwise until 5YR.

The *ad hoc* choice of radial segments is admittedly inelegant. It would have been preferable to make the segments either all linear, as Rheinboldt and Simon did, or all radial. Both these options were tried, however, and both resulted in small but noticeable errors. The routine `LinearVsRadialInterpOnRenotationOvoid.m` determines whether a segment is linear or radial. Since the program is open source, a user could easily add a few lines to this routine, so that it always specifies linear segments, or always specifies radial segments.

The ovoids are curves of constant chroma. Curves of constant hue will be drawn by linear interpolation between data points of the same hue, but consecutive chromas.

Figure 2 shows the ovoids and radials that result for Munsell value 4, when radial interpolation is used for the segments listed in 1, and linear interpolation is used for hue radials. Though not perfect, the ovoids are acceptably smooth. Similar figures can be drawn for any integer Munsell value, using Table 1.

Ovoids and radials collapse to a point in the special case of value 10. When Munsell value is 10, the only sample is a perfect reflecting diffuser, whose colour is an ideal white. The renotation figure corresponding to Figure 2 therefore consists of a single point,  $N 10/$ , whose chromaticity coordinates are given by Equations 7 and 8.

### 3.1.2 Interpolation with Ovoids and Radials

The previous constructions provide a model for some special cases. Let  $\{pH, V, C\}$  be a Munsell specification, where  $V$  is an integer and  $C$  is an integer multiple of

Value	Chroma	Radially Interpolated Hue Segments
1	2	10Y-5YR, 5P-10BG
	4	7.5Y-2.5YR, 10PB-7.5BG
	6	10PB-5BG
	8	7.5PB-7.5B
	$\geq 10$	7.5PB-2.5PB
2	2	7.5Y-5YR, 10PB-7.5PB
	4	10Y-2.5YR, 10PB-2.5B
	6	2.5Y-7.5R, 10PB-2.5B
	8	5YR-7.5R, 10PB-10BG
	$\geq 10$	7.5PB-5B
3	2	7.5GY-10R, 5P-5B
	4	7.5GY-5R, 2.5PB-5BG
	6, 8, 10	7.5GY-7.5R, 2.5P-7.5BG
	$\geq 12$	2.5G-7.5R, 10PB-7.5BG
4	2, 4	2.5G-7.5R, 5P-7.5BG
	6, 8	10GY-7.5R, 2.5P-7.5BG
	$\geq 10$	10GY-7.5R, 10PB-7.5BG
5	2	7.5GY-5R, 5P-5BG
	4, 6, 8	2.5G-2.5R, 5P-5BG
	$\geq 10$	2.5G-2.5R, 2.5P-5BG
6	2, 4	7.5GY-5R, 7.5P-5BG
	6	2.5G-5R, 7.5P-7.5BG
	8, 10	2.5G-5R, 5P-10BG
	12, 14	2.5G-5R, 2.5P-10BG
	$\geq 16$	2.5G-5R, 10PB-10BG
7	2, 4, 6	2.5G-5R, 5P-10BG
	8	2.5G-5R, 2.5P-10BG
	10	5Y-5R, 2.5G-10Y, 2.5P-10BG
	12	7.5Y-7.5R, 2.5G-10Y, 2.5P-10PB
	$\geq 14$	5YR-7.5R, 10GY-2.5GY, 2.5P-10PB
8	2, 4, 6, 8, 10, 12	10GY-5R, 5P-10BG
	$\geq 14$	5YR-5R, 10GY-2.5GY, 5P-10BG
9	2, 4	10GY-5R, 10PB-5BG
	6, 8, 10, 12, 14	2.5G-5R
	$\geq 16$	2.5G-5GY

Table 1: Radially Interpolated Hue Segments

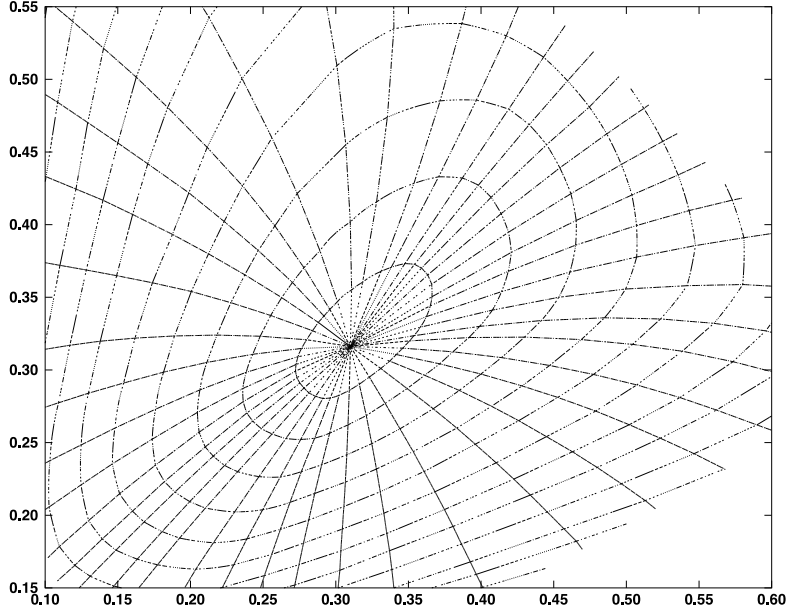


Figure 2: Interpolated Ovoids and Radials for Munsell Value 4

2, whose  $xy$  coordinates we want to calculate. This colour must lie on the ovoid of constant chroma  $C$ , in the plane with integer value  $V$ .  $pH$  should be between the two immediately adjacent hues for which renotation data is available:

$$p_1H_1 \leq pH \leq p_2H_2. \quad (17)$$

Inequality (17) requires a modular numbering scheme for standard Munsell hues, such as labeling them counterclockwise from 0 to 100, as suggested by Fig. 1 of the ASTM standard.<sup>3</sup>

$\{pH, V, C\}$  is on the ovoid between the two renotation points  $\{p_1H_1, V, C\}$  and  $\{p_2H_2, V, C\}$ . Transform these renotation points to polar coordinates, getting  $(r_1, \theta_1)$  and  $(r_2, \theta_2)$ , and also to  $xy$  coordinates, getting  $(x_1, y_1)$  and  $(x_2, y_2)$ . Since hues correlate approximately with polar angles, interpolate linearly to get the value of  $\theta$  that corresponds to  $\{pH, V, C\}$ :

$$\theta = \left( \frac{p_2H_2 - pH}{p_2H_2 - p_1H_1} \right) \theta_1 + \left( \frac{pH - p_1H_1}{p_2H_2 - p_1H_1} \right) \theta_2. \quad (18)$$

If the segment from  $\{p_1H_1, V, C\}$  to  $\{p_2H_2, V, C\}$  is interpolated radially, then, by construction, the corresponding point on the ovoid satisfies Equation (16), so the  $r$

corresponding to  $\{pH, V, C\}$  is given by

$$r = \left( \frac{\theta_2 - \theta}{\theta_2 - \theta_1} \right) r_1 + \left( \frac{\theta - \theta_1}{\theta_2 - \theta_1} \right) r_2. \quad (19)$$

If the segment from  $\{p_1H_1, V, C\}$  to  $\{p_2H_2, V, C\}$  is interpolated linearly, then the  $(x, y)$  is given by

$$(x, y) = \left( \frac{\theta_2 - \theta}{\theta_2 - \theta_1} \right) (x_1, y_1) + \left( \frac{\theta - \theta_1}{\theta_2 - \theta_1} \right) (x_2, y_2). \quad (20)$$

Equation (19) might have to be adjusted for wraparound, say if  $\theta_1$  were  $355^\circ$  and  $\theta_2$  were  $5^\circ$ . For radial interpolation, Expressions (18) and (19) can be converted to the  $xy$  coordinates for  $\{pH, V, C\}$ .

Similarly, suppose that  $\{pH, V, C\}$  is a Munsell specification for which  $V$  is an integer and  $pH$  is a standard Munsell hue. Choose two chromas that are even integers and are immediately adjacent to  $C$  :

$$C_1 \leq C \leq C_2. \quad (21)$$

Then  $\{pH, V, C\}$  lies on the radial containing  $\{pH, V, C_1\}$  and  $\{pH, V, C_2\}$ , with corresponding grid points  $(x_1, y_1)$  and  $(x_2, y_2)$ . The  $xy$  coordinates for  $\{pH, V, C\}$  can be found by linear interpolation.

Now combine the two previous cases into a more general case, assuming only that  $\{pH, V, C\}$  is a Munsell specification for which  $V$  is an integer.  $pH$  is still bounded by  $p_1H_1$  and  $p_2H_2$ , and  $C$  is bounded by  $C_1$  and  $C_2$ . The subscripted quantities define a quadrangle, like those appearing in Figure 2. Two sides of the quadrangle are given by chroma rings, and two are given by hue radials. The Munsell specification is within this quadrangle, or possibly on its boundary.

The two boundary points on the inner chroma ring correspond to the Table I values for  $\{p_1H_1, V, C_1\}$  and  $\{p_2H_2, V, C_1\}$ . From these locations, one can interpolate the position of  $\{pH, V, C_1\}$  on the inner ring. Similarly, one finds the position of  $\{pH, V, C_2\}$  on the outer ring. These two points have the desired hue,  $pH$ , so  $\{pH, V, C\}$  lies on the hue radial joining them. The point  $(x, y)$  for  $\{pH, V, C\}$  is found by linear interpolation along this radial, using the ratios of  $C$ ,  $C_1$ , and  $C_2$ .

### 3.2 Interpolation for Non-Integer Munsell Values

Section 3.1.2 shows how to interpolate over the Table I data, when the Munsell value is an integer. The current section shows how to interpolate for a Munsell

specification  $\{pH, V, C\}$ , where  $V$  is not an integer. The approach is similar. As long as  $V$  is between 1 and 10, it can be bounded by two adjacent integer values:

$$V_{\text{floor}} < V < V_{\text{ceil}}. \quad (22)$$

Since  $V_{\text{floor}}$  and  $V_{\text{ceil}}$  are integers, the previous section can be used to find their  $xyY$  coordinates,  $(x_{\text{floor}}, y_{\text{floor}}, Y_{\text{floor}})$  and  $(x_{\text{ceil}}, y_{\text{ceil}}, Y_{\text{ceil}})$ .

A natural approach, recommended by Newhall<sup>2</sup> (p. 407), Rheinboldt<sup>5</sup> (Fig. 2), Simon, and the ASTM, is linear interpolation over these two  $xyY$  conversions. In those papers, the interpolation was done using  $V$  rather than  $Y$ , because the quintic calculation to get  $Y$  from  $V$  was computationally demanding. Today, the quintic calculation is insignificant computationally, so it is used. The quantities  $Y$ ,  $Y_{\text{floor}}$ , and  $Y_{\text{ceil}}$ , are first obtained from  $V$ ,  $V_{\text{floor}}$ , and  $V_{\text{ceil}}$ , by Equation (12).  $Y$  is the  $Y$ -coordinate for  $\{pH, V, C\}$ .  $x$  and  $y$  are found by linear interpolation over the  $Y$ -values:

$$x = \left( \frac{Y_{\text{ceil}} - Y}{Y_{\text{ceil}} - Y_{\text{floor}}} \right) x_{\text{floor}} + \left( \frac{Y - Y_{\text{floor}}}{Y_{\text{ceil}} - Y_{\text{floor}}} \right) x_{\text{ceil}}, \quad (23)$$

$$y = \left( \frac{Y_{\text{ceil}} - Y}{Y_{\text{ceil}} - Y_{\text{floor}}} \right) y_{\text{floor}} + \left( \frac{Y - Y_{\text{floor}}}{Y_{\text{ceil}} - Y_{\text{floor}}} \right) y_{\text{ceil}}. \quad (24)$$

## 4 Renotation Inversion

Section 3 has described how to interpolate from the renotation data in Table I of Newhall's paper, to any Munsell specification. Algorithms have been provided for evaluating the function  $f$ , whose three subfunctions  $f_1$ ,  $f_2$ , and  $f_3$ , appear in Equations (9) through (11).

The current section is devoted to the inverse problem: how to go from  $xyY$  coordinates to Munsell coordinates,  $\{pH, V, C\}$ . The inverse will use the interpolation function  $f$  iteratively on a set of Munsell coordinates. For a given  $(x, y, Y)$ , multiple potential Munsell specifications will be constructed. When one is found such that  $f(pH, V, C)$  agrees with  $(x, y, Y)$  to within some tolerance, the iterations will terminate.

This approach differs from that of Newhall, Rheinboldt, and Simon. Rheinboldt used an exhaustive search to find the quadrangle containing  $(x, y)$ , for an appropriate integer Munsell value. Simon performed a similar exhaustive search for the quadrangle, but on a carefully chosen region that was much smaller. Newhall recommended a graphical method, in which the quadrangle would be visually located on the plots provided. Since Rheinboldt's and Simon's quadrangles were based on

linear rather than radial interpolation, it was not too computationally demanding to invert linearly to find Munsell hue and chroma.

An example will illustrate the iterative method used in this paper. Let  $(x, y, Y)$  be the point  $(0.52, 0.27, 11.71)$ , for which the Munsell coordinates are desired.

#### 4.1 Munsell Value Calculation

First, invert Equation (12) to find that the value  $V$  is the integer 4. Although the ASTM recommends an analytic expression from McCamy,<sup>10</sup> a lookup table provides a more accurate inversion, at minimal computational cost. McCamy's expression approximates  $f_1^{-1}$ , which should satisfy  $f_1^{-1}(f_1(V)) = V$  and  $f_1(f_1^{-1}(Y)) = Y$ . In the current example,  $f_1(f_1^{-1}(11.710)) = 11.702$  when McCamy's expression is used, and 11.710 when the lookup table is used.

The lookup table method precomputes Equation (12) at Munsell values, from 0 to 10 in increments of 0.02, producing 501 monotonically increasing luminance factors. The method finds the two luminance factors immediately bounding a given  $Y$ , and interpolates linearly to get the corresponding Munsell value. To compare the two methods, the absolute errors,  $|f_1^{-1}(f_1(V)) - V|$ , were calculated for 1000 randomly chosen Munsell values. (Random selection eliminates any artifacts of the lookup table.) Figure 3 plots the results.

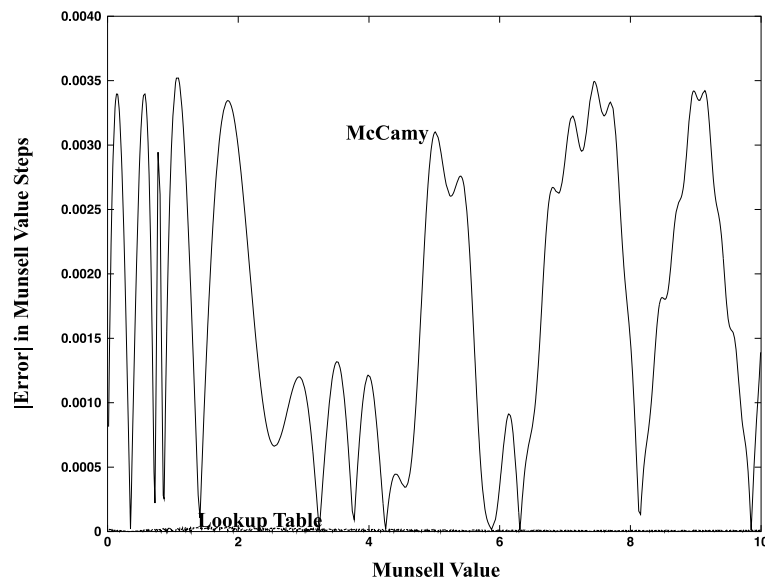


Figure 3: Errors in McCamy's Expression, vs Errors in Lookup Table Method

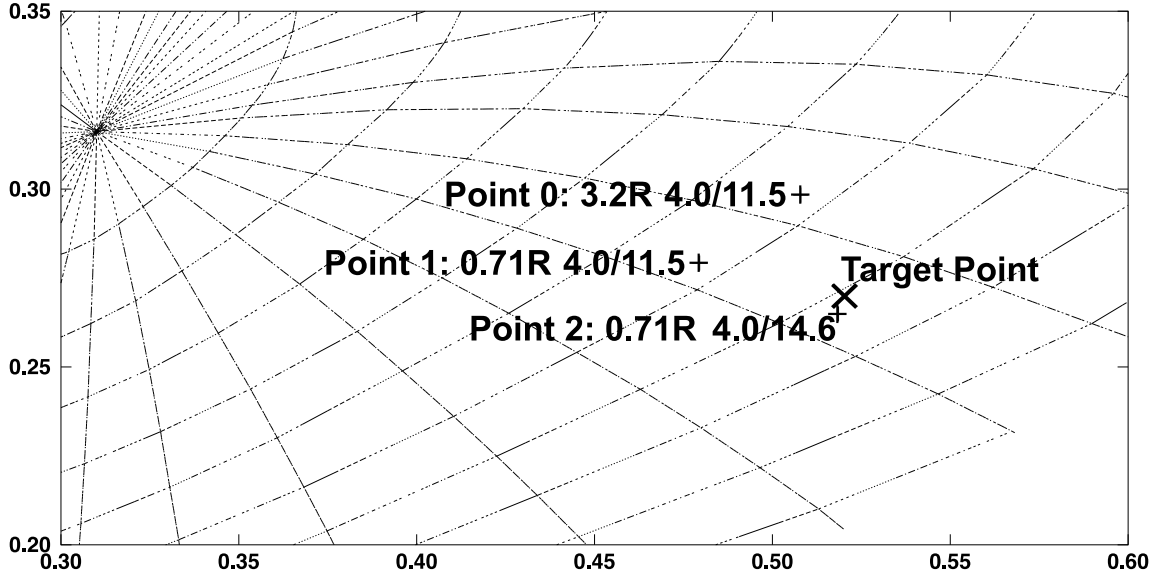


Figure 4: Target Point and Intermediate Points for Inversion Example

Ideally, the absolute values of the errors should be 0. McCamy’s errors are on the upper line, not exceeding 0.0035. The lookup table errors, however, are less than 1% of McCamy’s, not exceeding  $3.2 \times 10^{-5}$ . In any single calculation, both methods are accurate enough, and agree to at least three significant digits. The lookup table method was preferred here, so that converting from  $xyY$  to Munsell, and then back to  $xyY$  again, would be accurate to four significant digits, which is the maximum precision of  $f_1$ , according to Sect. 8.6 of the ASTM standard.<sup>3</sup>

Now that the Munsell value 4 has been calculated, we can use the ovoids and radials in Figure 2. Even if  $V$  were not an integer, there would still be a set of ovoids and radials corresponding to  $V$ , similar to Figure 2, which we could use. Figure 4 shows the target point as an X. Converting it to polar coordinates around the white point gives the target coordinates

$$(r_{\text{tar}}, \theta_{\text{tar}}) = (0.215, 347.6^\circ). \tag{25}$$

By iteration, we will find a Munsell specification that  $f$  maps to  $(r_{\text{tar}}, \theta_{\text{tar}})$ .

## 4.2 The Initial Approximation

Use the CIELAB model (Sect. 10.3 of Ref. 11) to start the iterative process. CIELAB takes  $XYZ$  coordinates as input, so  $(x, y, Y)$  must be first converted to  $(X, Y, Z)$ ,

using Equations (4) to (6). Two outputs of the CIELAB model are a hue angle ( $h^*$ ) and a chroma correlate ( $C^*$ ).  $h^*$  corresponds roughly to a Munsell hue, as seen in Fig. 10.4 of Ref. 11.  $C^*$  is usually between 4.5 and 5.5 times the Munsell chroma. We divide  $C^*$  by 5.5 to get an approximate Munsell chroma. The result in the case given is 3.2R 4.0/11.5. The Section 3 interpolation evaluates  $f$  at this Munsell specification, producing the  $xyY$  coordinates shown as Point 0 in Figure 4. Point 0 is the initial approximation to the target point. Its polar coordinates are

$$(r_0, \theta_0) = (0.20, 354.6^\circ). \quad (26)$$

The inversion algorithm will iteratively modify the initial point until it matches the target point sufficiently closely. The modifications will alternate between hue ( $\theta$ ) modifications and chroma ( $r$ ) modifications. An iteration for this algorithm will be defined as the combination of a hue modification and the consecutive chroma modification.

### 4.3 The Hue Modification Step

Start with a  $\theta$  modification.  $\theta_0$  is about  $7^\circ$  past  $\theta_{\text{tar}}$ . It would be desirable to modify  $\theta_0$  by shifting it about  $7^\circ$  clockwise. This operation cannot be performed directly, because the hue radials curve slightly rather than being straight. From Figure 2, the hue radial corresponding to 3.2R makes an angle just above  $0^\circ$  at the origin, and then curves downward to intersect the straight radial of angle  $354.6^\circ$  at the initial approximation point. The hue radial angle should therefore be adjusted by adding  $7^\circ$  in the clockwise direction.

This addition requires a mapping of hues to hue angles. The mapping is somewhat arbitrary, but should be used consistently. The current implementation, for example, defined 5R to have a hue angle of  $0^\circ$ , and 5P to have a hue angle of  $315^\circ$ . The hue 10P, which is halfway between 5R and 5P in the Munsell system, would then have a hue angle of  $337.5^\circ$ , and other intermediate hues could be assigned hue angles similarly; in this case, the hue angle for 3.2R is  $352.1^\circ$ . The mapping of hues to hue angles was motivated by the chromaticity diagram, and is consistent with Figures 1 through 9 of the renotation.<sup>2</sup> The mapping is invertible. Moving  $7^\circ$  clockwise from the hue angle for 3.2R results in a new hue angle,  $345.1^\circ$ , which corresponds to 1.7R.

The hue of the initial Munsell specification is adjusted, giving a new specification, 1.7R 4.0/11.5, which  $f$  maps to  $(0.18, 350.2^\circ)$ . The target  $\theta$  value is  $347.6^\circ$ , which is not between  $350.2^\circ$  and  $354.6^\circ$ . The process of subtracting  $7^\circ$  is repeated, giving a new hue angle of  $338.1^\circ$ , and a new hue of 0.1R.  $f$  maps the specification 0.1R 4.0/11.5 to  $(0.17, 345.8^\circ)$ .  $\theta_{\text{tar}}$  is between  $345.8^\circ$  and  $350.2^\circ$ , slightly nearer  $345.8^\circ$ . The hue for

the inversion's next approximation to the target point is therefore between 0.1R (the hue for  $345.8^\circ$ ) and 1.7R (the hue for  $350.2^\circ$ ), but slightly nearer 0.1R. The precise hue is found by linear interpolation on the hues, giving 0.76R in this instance. The second Munsell specification in the iteration is 0.76R 4.0/11.5, with polar coordinates

$$(r_1, \theta_1) = (0.176, 347.6^\circ). \quad (27)$$

This point appears as Point 1 in Figure 4. Point 0 and Point 1 are on the same ovoid, but the hue of Point 1 more closely matches the hue of the target point.

The net effect of the hue adjustment step is a Munsell specification whose  $\theta$  value is closer to the target  $\theta$  value than the initial approximation. In the example just given, two adjustments, of  $7^\circ$  each, were needed to bound  $\theta_{\text{tar}}$  in both the clockwise and counterclockwise directions. In almost all cases, two adjustments are sufficient, and often only one is necessary; more can be taken if required. Note that the distance from Point 1 to the target might actually be greater than the distance from Point 0 to the target, so the inversion algorithm is temporarily farther from its target point. While this happens occasionally, the algorithm generally converges quickly.

#### 4.4 The Chroma Modification Step

The hue modification step adjusted the hue of the current Munsell specification, without adjusting its chroma. In this step, we adjust the chroma and leave the hue alone. Geometrically, hue corresponds to  $\theta$  and chroma corresponds to  $r$ , so the chroma step moves the specification nearer the target, approximately along a radial from the white point.

The approach is similar to the hue modification step. The current Munsell specification, given by Equation (27), has an  $r$  value,  $r_1$ , that differs from the value of  $r_{\text{tar}}$  in Equation (25). Increase the chroma, 11.5, of the current Munsell specification, by a factor of

$$\frac{r_{\text{tar}}}{r_1} = \frac{0.215}{0.176} = 1.22, \quad (28)$$

giving a new chroma of  $1.22 \times 11.5 = 14.0$ .  $f(0.71\text{R } 4.0/14.0)$  is  $(0.210, 346.3^\circ)$ , in polar coordinates. The new  $r$  value is just short of  $r_{\text{tar}}$ , so multiply the chroma by 1.22 again, getting another Munsell specification, 0.71R 4.0/17.1. This time,

$$f(0.71\text{R } 4.0/17.1) = (0.250, 344.9^\circ). \quad (29)$$

The desired  $r_{\text{tar}}$  is 0.215, which is between the  $r$  values of 0.210 (corresponding to the chroma 14.1) and 0.250 (corresponding to the chroma 17.3), but much nearer the first

$r$  value. By linear interpolation, the chroma corresponding to 0.215 is 14.6. Define Point 2 in the iterative sequence to be 0.71R 4.0/14.6. Applying the interpolation function  $f$  gives

$$(r_2, \theta_2) = (0.215, 346.2^\circ). \quad (30)$$

Point 2 appears in Figure 4. Point 1 and Point 2 are on the same hue radial, but the chroma of Point 2 is closer to the chroma of the target point.

#### 4.5 Alternating Hue and Chroma Steps, and Termination

Figure 4 shows that Point 2 is already close to the target point. Further iterations consist of pairs of hue and chroma adjustment. The hue-chroma iterations continue until the point produced is within a certain tolerance,  $\epsilon$ , of the target point.  $\epsilon$  is measured with respect to the Euclidean distance in  $x$  and  $y$ . In the calculations for this paper,  $\epsilon$  was set to 0.0001. In the current example, the algorithm terminated after four iterations, giving a Munsell specification of 1.14R 4.00/14.18.

Although not implemented here, other termination criteria could use the Munsell quantities directly. For example, iterations could be run until three hues, from three consecutive iterations, all agreed to within two significant digits, thus insuring that the Munsell colour had a desired hue accuracy. Similar conditions could be placed on the chromas, or on hues and chromas jointly. (The Munsell value, of course, is already completely determined by  $Y$ .)

#### 4.6 The MacAdam Limits

Not every combination of values for  $x$ ,  $y$ , and  $Y$ , determines a physically realizable colour. The Munsell renotation extends only to the MacAdam limits, which are the boundaries between realizable and non-realizable colours. The empty areas in Figure 2, for example, are outside the MacAdam limits, so have no corresponding Munsell coordinates. The inverse renotation is not defined in the empty regions, either. The inversion algorithm, however, sometimes requires a chroma or hue that is beyond the MacAdam limits. When needed, the Munsell renotation was extrapolated beyond the 1943 values, using values provided by the Munsell Color Science Laboratory.<sup>12</sup>

The MacAdam limits for the inverse renotation were calculated from Table II of MacAdam's 1935 paper,<sup>13</sup> which lists optimal colours with regard to Illuminant C. The convex hull of the table entries (when converted to CIE  $XYZ$  coordinates), along with additional entries for theoretical black and white, was taken to define the set of possible object colours. Any  $xyY$  specification which, when converted to an  $XYZ$

specification, was not within the convex hull, was taken to be outside the MacAdam limits. The smallest luminance factor for an optimal colour in MacAdam's table is 10%, which corresponds to a Munsell value of about 3.5, so the inverse renotation might not reach the MacAdam limits for some lower value entries.

## 4.7 Inversion Algorithm Performance

In practice, the inversion algorithm usually calculated no more than half a dozen hue-chroma iterations before successfully terminating. Typically, as in Figure 4, very good convergence had already occurred by the first or second iteration. In general, each iteration seemed to reduce the Euclidean distance between the target colour and the new estimate by nearly an order of magnitude. No attempt was made to optimize the algorithm. The inversion algorithm can be run from the command line in Matlab or Octave. If one enters

```
> MunsellSpecification = xyYtoMunsell(0.52, 0.27, 11.71)
```

then the routine returns

```
MunsellSpecification = 1.14R4.00/14.18.
```

Conversely, entering

```
> [x y Y] = MunsellToxyY('1.14R4.00/14.18')
```

returns

```
x = 0.51999,  
y = 0.27002,  
Y = 11.701.
```

Apart from running cases one at a time on the command line, Octave scripts can be written that will automatically run many cases, and record the output.

From one point of view, the inversion algorithm is irrelevant. If  $f(\{pH, V, C\})$  agrees with the desired  $(x, y, Y)$ , to within an acceptable tolerance, then the inversion has been successful, regardless of the algorithm used. As implemented, the inversion routine, `xyYtoMunsell.m`, makes numerous calls to the interpolation routine, `MunsellToxyY.m`, but not vice versa. If the interpolation method were modified, the inversion routine would adapt automatically, without requiring any modification itself. The important question is therefore how to extend the Munsell renotation from the colours listed in Table I of the 1943 paper,<sup>2</sup> to unlisted colours.

	$x$	$y$	$Y$	Previous Inversion	Current Inversion	Hue Diff.	Value Diff.	Chroma Diff.
Simon & Frost	0.1988	0.1930	8.39	4.53PB 3.39/7.86	4.58PB 3.43/7.76	0.05	0.04	0.10
	0.3352	0.2404	7.67	1.09RP 3.24/5.91	1.13RP 3.28/5.94	0.04	0.04	0.03
	0.4784	0.3095	11.05	4.24R 3.85/8.72	3.89R 3.90/8.86	0.35	0.05	0.14
	0.4385	0.4824	28.63	7.88Y 5.88/8.68	7.81Y 5.94/8.74	0.07	0.06	0.06
	0.5190	0.3695	15.13	1.36YR 4.44/9.35	1.12YR 4.49/9.41	0.24	0.05	0.06
	0.5184	0.3573	6.20	1.38YR 2.92/6.90	1.10YR 2.95/6.99	0.28	0.03	0.09
	0.2687	0.2842	13.54	0.30PB 4.23/2.59	0.59PB 4.27/2.59	0.29	0.04	0.00
	0.3036	0.3747	3.18	10.00GY 2.02/2.52	0.23G 2.05/2.54	0.23	0.03	0.02
	0.3517	0.3492	12.76	0.42Y 4.11/1.54	0.42Y 4.16/1.54	0.00	0.05	0.00
	0.3421	0.3252	18.55	9.37R 4.86/1.75	9.29R 4.92/1.76	0.08	0.06	0.01
	0.3767	0.3546	12.88	7.19YR 4.13/2.45	6.84YR 4.18/2.48	0.35	0.05	0.03
	0.2697	0.2640	14.89	6.63PB 4.41/3.69	6.63PB 4.46/3.66	0.00	0.05	0.03
	0.2882	0.3492	28.41	6.18G 5.86/3.28	6.24G 5.92/3.30	0.06	0.06	0.02
	0.3918	0.3800	30.97	0.28Y 6.08/4.30	9.83YR 6.14/4.36	0.45	0.06	0.06
	0.3099	0.3153	16.02	N 4.56/	N 4.61/	-	0.05	-
	0.2665	0.3291	25.71	4.14BG 5.61/3.82	4.13BG 5.67/3.84	0.01	0.06	0.02
	0.3952	0.3084	8.75	2.36R 3.45/4.26	2.30R 3.50/4.20	0.06	0.05	0.06
ASTM	0.2395	0.2905	59.53	3.9B 8.11/6.6	4.00B 8.11/6.59	0.10	0.00	0.01
	0.3434	0.3025	80.84	5.9RP 9.19/6.0	6.08RP 9.19/6.63	0.18	0.00	0.63
	0.4183	0.3790	72.22	5.4YR 8.78/7.6	5.41YR 8.78/7.58	0.01	0.00	0.02
	0.4690	0.4953	50.30	5.6Y 7.56/13.7	5.57Y 7.56/13.63	0.03	0.00	0.07
Walkill	0.3434	0.3025	80.84	5.9RP 9.19/5.60	6.08RP 9.19/6.63	0.18	0.00	1.03
	0.1600	0.1900	1.79	8.34B 1.40/5.38	8.19B 1.40/5.21	0.15	0.00	0.17
	0.2700	0.3100	7.76	8.53BG 3.30/2.04	8.53BG 3.30/2.00	0.00	0.00	0.04
	0.4200	0.3600	19.77	2.75YR 5.06/5.28	2.77YR 5.06/5.26	0.02	0.00	0.02
	0.2800	0.2500	31.62	1.99P 6.20/6.71	1.96P 6.20/6.67	0.03	0.00	0.04
	0.3200	0.5400	47.86	9.29GY 7.40/13.79	9.24GY 7.40/13.65	0.05	0.00	0.14

Table 2: Comparative Output of Different Inversion Algorithms

Table 2 compares inversions calculated by the current method, with inversions calculated by previous methods. The first 17 examples are taken from Table I of Simon & Frost,<sup>6</sup> the next four are from Table 4 of the ASTM standard.<sup>3</sup> The final six were obtained from Walkill.<sup>7</sup> The Walkill program was run with Illuminant C and the 1931 2° observer selected. In addition, the box marked “PWD” was checked; running without the PWD box checked seemed to make Walkill use Newhall’s quintic, while running with it checked seemed to make it use the ASTM quintic. For each  $xyY$  combination, the table lists the Munsell specification calculated by a previous inversion, and the specification calculated by the current inversion. The final three columns of the table list the differences in hue, value, and chroma, between the two specifications.

There is a slight but consistent value difference between Simon’s results and the current results. This difference occurs because Simon used the inverse of Newhall’s quintic, rather than the updated ASTM quintic. The difference is more pronounced when Munsell value is higher; Simon’s examples do not exceed 6 in value, so the difference is not great. Since Simon interpolates between value planes, a difference in value leads to differences in hue and chroma. While the chroma differences in Simon’s cases would probably not be discernible, some of the hue differences, exceeding a quarter of a hue step, would be.

Table 3 shows an attempt to reproduce Simon’s results, by modifying the current

$x$	$y$	$Y$	Graphical Inversion	Simon's Inversion	Current Inversion	Modified Inversion
0.1988	0.1930	8.39	4.72PB 3.38/7.90	4.53PB 3.39/7.86	4.58PB 3.43/7.76	4.59PB 3.38/7.78
0.3352	0.2404	7.67	1.15RP 3.24/5.95	1.09RP 3.24/5.91	1.13RP 3.28/5.94	1.13RP 3.24/5.93
0.4784	0.3095	11.05	4.00R 3.85/8.89	4.24R 3.85/8.72	3.89R 3.90/8.86	3.91R 3.85/8.79
0.4385	0.4824	28.63	7.79Y 5.88/8.68	7.88Y 5.88/8.68	7.81Y 5.94/8.74	7.82Y 5.88/8.67
0.5190	0.3695	15.13	1.12YR 4.44/9.40	1.36YR 4.44/9.35	1.12YR 4.49/9.41	1.10YR 4.44/9.41
0.5184	0.3573	6.20	1.14YR 2.92/6.93	1.38YR 2.92/6.90	1.10YR 2.95/6.99	1.11YR 2.92/6.97
0.2687	0.2842	13.54	0.77PB 4.23/2.38	0.30PB 4.23/2.59	0.59PB 4.27/2.59	0.59PB 4.23/2.58
0.3036	0.3747	3.18	0.38G 2.02/2.55	10.00GY 2.02/2.52	0.23G 2.05/2.54	0.22G 2.02/2.54
0.3517	0.3492	12.76	0.50Y 4.11/1.50	0.42Y 4.11/1.54	0.42Y 4.16/1.54	0.42Y 4.11/1.54
0.3421	0.3252	18.55	9.37R 4.86/1.82	9.37R 4.86/1.75	9.29R 4.92/1.76	9.27R 4.86/1.74
0.3767	0.3546	12.88	6.60YR 4.13/2.51	7.19YR 4.13/2.45	6.84YR 4.18/2.48	6.82YR 4.13/2.47
0.2697	0.2640	14.89	6.26PB 4.41/3.51	6.63PB 4.41/3.69	6.63PB 4.46/3.66	6.65PB 4.41/3.65
0.2882	0.3492	28.41	5.93G 5.86/3.25	6.18G 5.86/3.28	6.24G 5.92/3.30	6.26G 5.86/3.29
0.3918	0.3800	30.97	9.97YR 6.08/4.48	0.28Y 6.08/4.30	9.83YR 6.14/4.36	9.83YR 6.08/4.34
0.3099	0.3153	16.02	N 4.56/	N 4.56/	N 4.61/	N 4.56/
0.2665	0.3291	25.71	4.03BG 5.61/3.82	4.14BG 5.61/3.82	4.13BG 5.67/3.84	4.11BG 5.61/3.83
0.3952	0.3084	8.75	2.15R 3.45/4.27	2.36R 3.45/4.26	2.30R 3.50/4.20	2.29R 3.45/4.21

Table 3: Comparison with Simon's Output

inversion. The following changes were made: the value conversion used Newhall's quintic instead of the ASTM quintic, interpolation was done over Munsell value rather than over  $Y$ , and all interpolations were linear rather than radial. Table 3 also shows the results of graphical inversion, taken from Table I of Simon's 1987 paper. In theory, Simon's inversion should agree with the modified inversion. In fact, Table 3 shows significant discrepancies. Although the Munsell values agree (as they must), the modified inversion matches the graphical inversion in hue better than Simon's inversion, in all but three cases. In the third row, for example, the modified and graphical inversions differ in hue by 0.09 Munsell steps, while Simon's and the graphical inversion differ by 0.24 Munsell steps. Chroma discrepancies follow a similar pattern, though not as pronounced. The inability to reproduce Simon and Frost's results probably cannot be explained without a source code comparison; a numerical implementation difference might be producing the differences seen in the table.

By contrast with Simon's results, there is much less difference between ASTM's results, Wallkill's result, and the current result. The Munsell values are identical because the ASTM algorithm, and presumably Wallkill's algorithm, both use McCamy's analytic approximation to calculate  $V$  from  $Y$ , and the current lookup table approach produces only negligibly different results. In three of the ASTM cases, both hue and chroma differences are slight. They probably result from the fact that ASTM interpolates over  $V$ , while the current method interpolates over  $Y$ , as explained in Section 3.2. In addition, of course, the graphical interpolations recommended by the ASTM introduce some error, which can account for the differences.

One striking difference occurs when  $xyY = (0.3434, 0.3025, 80.84)$ . In this case, the chroma difference is 0.63. Technically, the ASTM algorithm should not be able

to invert this  $xyY$  combination. Sect. 8.1 of the ASTM standard<sup>3</sup> gives inversion instructions resulting in a Munsell value of 9.19. Sect. 8.2 then says to estimate hue and chroma at  $(x, y)$ , from the figures for the bounding values, 9 and 10. There is, however, no figure corresponding to value 10. Even if there were, it would be impossible to estimate hue and chroma from it, as all hues and chromas at value 10 are mapped to one point, the Illuminant C chromaticity point. While there are geometrically reasonable inversion methods for Munsell values greater than 9, the ASTM does not specify any, so their conversion, and its difference from the open-source conversion, will be disregarded.

The table shows a more serious discrepancy when Wallkill is run on this case. The current algorithm's chroma differs from Wallkill by 1.03. Wallkill's chroma also differs from the ASTM chroma by a significant 0.40. To investigate the effect of interpolating over  $Y$ , versus interpolating over  $V$ , the current algorithm was run again, interpolating over  $V$  rather than  $Y$ . The new specification was 6.10RP 9.19/6.75, an even larger difference. Since the Wallkill algorithm is unknown, this discrepancy is hard to explain. When a colour's Munsell value exceeds 9, interpolation is tricky, because there is only one data point, ideal white, of value 10. A radically different interpolation scheme on Wallkill's part, or additional renotation data, might explain the discrepancy, but a definite answer would require information about the Wallkill algorithm. As a caution, one could restrict the current inversion to values no greater than 9. The current inversion will not return an answer for values less than 1, so there are no similar concerns for very dark values.

Three of the remaining five Wallkill examples show very good agreement, with differences less than 0.05 for both hue and chroma. Algorithm differences account for the moderately large differences seen in the other two examples. The current algorithm was rerun on the case  $xyY = (0.16, 0.19, 1.79)$ , but modified so that interpolation was done over Munsell value, instead of over luminance factor; the result was 8.23B 1.40/5.34, reducing the chroma difference to 0.04, and the hue difference to 0.11. The last example on the table is probably due to differences in the ovoid approximation. The ovoid segments between 7.5GY and 10 GY, for values between 7 and 8, and chromas greater than 12, show high curvature. While a radial interpolation of these segments, which is used here, is preferable to a linear interpolation, the Wallkill program might use other methods, such as splines or Bézier curves, to match the plots in the original paper.<sup>2</sup> A definite answer would require knowledge of the Wallkill algorithm. In general, however, the ovoids' form between data points comes from an *ad hoc* visual estimate, rather than a calculation. Considering the high curvature in this case, a difference of 0.14 chroma steps is within reasonable estimation error.

In general, for Munsell values between 1 and 9, the current algorithm's hues and chromas, as shown in Table 2, differ by less than 0.1 from the two most recent algorithms, and internal details of the algorithms can explain most of the differences. Human wavelength discrimination<sup>14</sup> for monochromatic stimuli in the visual spectrum, between 400 and 700 nm, is at best about 1 nm, and often considerably worse. A human could therefore distinguish no more than 300 hues in the visible spectrum. The visible spectrum extends about three quarters of the way around the Munsell hue circle, which is evenly spaced perceptually, so a human could distinguish no more than 400 Munsell hues. One four-hundredth of the hue circle corresponds to a Munsell hue difference of 0.25, so the Table 2 hue differences are imperceptible. Similarly, chroma discrimination data<sup>14</sup> shows that the chroma differences are also imperceptible.

Since the eye cannot distinguish the results of current algorithms, further algorithm refinement would provide limited benefit. The main contribution of the algorithm presented here is not its details, but its openness. It is hoped that other colour researchers will use the implementation freely, and adapt it to their needs.

1. Deane B. Judd. "The 1931 I. C. I. Standard Observer and Coordinate System for Colorimetry," *JOSA*, Vol. 23, October 1933, pp. 359-374.
2. Sidney Newhall, Dorothy Nickerson, & Deane B. Judd. "Final Report of the O. S. A. Subcommittee on the Spacing of the Munsell Colors," *JOSA*, Vol. 33, Issue 7, 1943, pp. 385-418.
3. ASTM Standard D 1535-08. "Standard Practice for Specifying Color by the Munsell System," 2008.
4. <http://www.uv.es/vista/vistavalencia/software/colorlab.html>, as of January 14, 2011.
5. Werner C. Rheinboldt & John P. Menard. "Mechanized Conversion of Colorimetric Data to Munsell Renotations," *JOSA*, Vol. 50, Number 8, 1960, pp. 802-817.
6. Frederick T. Simon & Judith A. Frost. "A New Method for the Conversion of CIE Colorimetric Data to Munsell Notations," *COLOR Research and Application*, Vol. 12, Number 5, 1987, pp. 256-260.
7. WallkillColor Munsell Conversion Software, available as of 8 January 2011 at <http://www.WallkillColor.com>.
8. BabelColor PatchTool Software, available as of 7 May 2011 at <http://www.babel-color.com/index.htm#PatchTool>.
9. N. S. Smith, T. W. A. Whitfield, & T. J. Wiltshire, "A Colour Notation Conversion Program," *COLOR Research and Application*, Vol. 15, Number 6, December 1990, pp. 338-343.

10. C. S. McCamy. "Munsell Value as Explicit Functions of CIE Luminance Factor," *COLOR Research and Application*, Vol. 17, 1992, pp. 205-207.
11. Mark D. Fairchild. *Color Appearance Models*, 2<sup>nd</sup> ed., John Wiley & Sons, Ltd, 2005.
12. <http://www.cis.rit.edu/mcsl/online/munsell.php/all.dat>, as of June 12, 2010.
13. David L. MacAdam. "Maximum Visual Efficiency of Colored Materials," *JOSA*, Vol. 25, Issue 11, 1935, pp. 361-367.
14. Yves Le Grand. *Light, Colour and Vision*, 2<sup>nd</sup> ed., Chapman & Hall, Ltd, 1968, Ch. 12.